

# The Gas-Phase Hydrogen-Bonded Complex between Ozone and Hydroperoxyl Radical. A Theoretical Study

Alex Mansergas and Josep M. Anglada\*

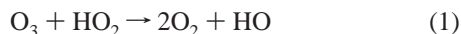
*Theoretical and Computational Chemistry Group, Departament de Química Orgànica Biològica, Institut d'Investigacions Químiques i Ambientals de Barcelona, IIQAB – CSIC, c/ Jordi Girona 18, E-08034 Barcelona, Spain*

*Received: September 22, 2006; In Final Form: November 23, 2006*

We report a theoretical study on the gas-phase hydrogen-bonded complexes formed between ozone and hydroperoxyl radical, which are of interest in atmospheric chemistry. We have employed CASSCF, CASPT2, QCISD, and CCSD(T) theoretical approaches employing 6-311+G(2df,2p) and aug-cc-pVTZ basis sets, and we have found three complexes whose stabilities are computed to be 2.02, 1.19, and 1.34 kcal/mol, respectively, at 0 K. In addition, we have also found three transition states connecting these complexes that lie below the energy of the separate reactants. To help for possible experimental identification of these hydrogen-bonded complexes, we report also the computed harmonic vibrational frequencies along with the frequency shifts of the complexes, relative to the monomers, and the computed rotational constants.

## Introduction

The reaction of hydroperoxyl radical with ozone (eq 1) is of great importance in both the troposphere and the stratosphere, as it participates in the ozone-destruction process.<sup>1–3</sup>



The rate constant of eq 1 has been measured by several authors and exhibits a non-Arrhenius behavior at low temperatures.<sup>4–9</sup> Regarding the reaction mechanism, Nelson and Zahniser,<sup>7</sup> measured product branching ratios at different temperatures using oxygen isotope labeling and concluded that hydrogen abstraction by ozone is the dominant pathway. However, a dynamical study by Varandas and Zhang<sup>10</sup> suggested that the reaction occurs via oxygen abstraction, and the discrepancy on the mechanism was tentatively attributed to isotope scrambling reactions. These results suggest the need of performing a further theoretical study on this reaction, and we have considered that the first stage of the reaction would involve the formation of pre-reactive hydrogen-bonded complex between ozone and hydroperoxyl radical, in a similar way as a pre-reactive hydrogen-bonded complex has been recently measured and characterized between O<sub>3</sub> and HO radical.<sup>11–13</sup> The existence of pre-reactive complexes has proven to be very useful to the understanding of the kinetic behavior of many gas-phase atmospheric reactions,<sup>14</sup> and we report in this work a theoretical study on the hydrogen-bonded complexes formed between O<sub>3</sub> and HO<sub>2</sub>, which is part of an ongoing ab initio study on this reaction. We have employed high-level ab initio calculations to locate and characterize these hydrogen-bonded complexes, to estimate its energetic stability, and to calculate the IR spectrum. By comparing the changes in the vibrational spectrum originated by the formation of the complexes, we aim to provide information that can be very useful in their possible experimental characterization.

## Computational Methods

All geometry optimizations have been carried out by using the 6-311+G(2df,2p)<sup>15,16</sup> basis set. In a first step, we have employed the complete active self-consistent field (CASSCF) method<sup>17</sup> to optimize and characterize all the stationary points. In these calculations, we have employed two different active spaces to construct the CASSCF wave function. Thus, for the hydrogen-bonded complexes, we have distributed 15 electrons in 13 orbitals (CASSCF(15,13)) and 19 electrons in 15 orbitals (CASSCF(19,15)); for O<sub>3</sub>, we have considered a CASSCF(12,9) active space and for HO<sub>2</sub> we have employed a CASSCF(7,6) active space. The composition of these active spaces was chosen according to the fractional occupation of the natural orbitals<sup>18</sup> generated from a first-order density matrix obtained from a multireference wave function (MRCI) correlating all valence electrons. A schematic description of them is given as Supporting Information.

The effect of the dynamical correlation energy on the relative stability of the stationary points was considered by carrying out CASPT2<sup>19</sup> single-point energy calculations on the basis of a common CASSCF(19,15) reference function with the 6-311+G(2df,2p) basis set.

It is well-known that the CASSCF wave functions do not properly describe hydrogen bond interactions because of the lack of consideration of the dynamical correlation energy. Therefore, in a second step, we have reoptimized and characterized the reactants and hydrogen-bonded complexes employing the single-determinant-based QCISD approach<sup>20</sup> with the 6-311+G(2df,2p) basis set. In addition, we have performed CCSD(T)<sup>21–24</sup> single-point energy calculations at the QCISD optimized geometries to consider the effect of higher (triple) excitations in the wave function to the energy. In these single-point energy calculations, we have employed the aug-cc-pVTZ<sup>25,26</sup> basis set. For these calculations, we have considered the value of the T1 diagnostic<sup>27,28</sup> of the CCSD wave function to assess the reliability of these calculations with regard to the multireference character of the wave function. For **C1**, **C2**, and **C3**, we have obtained T1 diagnostic values of 0.030, which are

\* To whom correspondence should be addressed. E-mail: anglada@iiqab.csic.es.

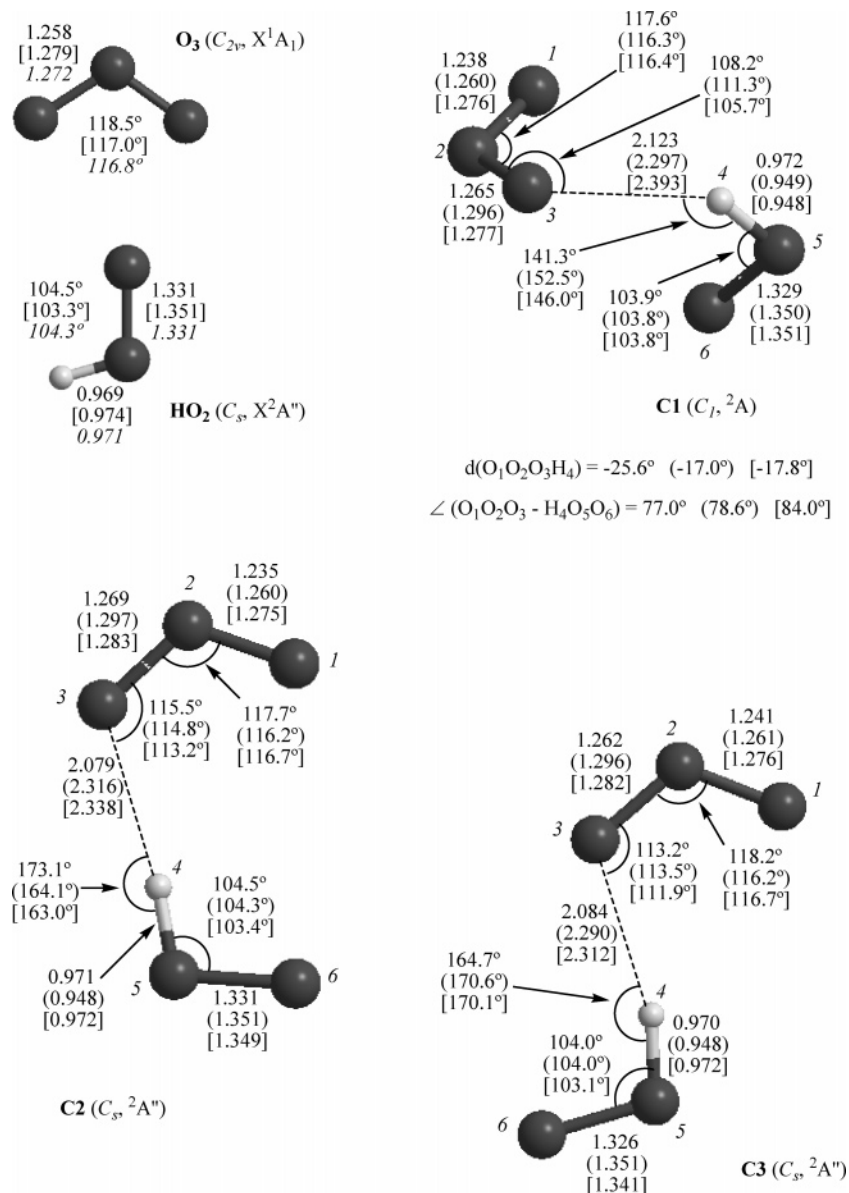


**Figure 1.** Selected geometrical parameters for the stationary points: for C1, C2, and C3, optimized at QCISD/6-311+G(2df,2p); CASSCF(15,-13)/6-311+G(2df,2p), in parentheses; and CASSCF(19,15)/6-311+G(2df,2p), in brackets; for O<sub>3</sub>, QCISD/6-311+G(2df,2p) and CASSCF(12,9)/6-311+G(2df,2p), in brackets; for HO<sub>2</sub>, QCISD/6-311+G(2df,2p) and CASSCF(7,6)/6-311+G(2df,2p), in brackets. For O<sub>3</sub> and HO<sub>2</sub>, the experimental values are given in italics.

in the range of the values suggested by Rienstra-Kiracofe and co-workers,<sup>28</sup> and therefore we are confident in the reliability of the QCISD and CCSD(T) calculations. Moreover, and to check the influence for the triple excitations in the hydrogen bond, we have also performed, for the most stable complex, a CCSD(T) optimization employing the 6-311+G(2df,2p) basis set, restricted to the most significant geometrical parameters regarding the hydrogen bond.

Finally, the stability of the complexes has been corrected by computing, at CCSD(T) and CASPT2(19,15) levels of theory, the basis set superposition error (BSSE) according to the counterpoise method by Boys and Bernardi.<sup>29</sup>

Moreover, the bonding features of the hydrogen bond interaction have been analyzed according to the atoms in molecules (AIM) theory by Bader.<sup>30</sup>

The harmonic vibrational frequencies and zero-point energies (ZPE) have been calculated at CASSCF(15,13)/6-311+G(2df,-2p), CASSCF(19,15)/6-311+G(2df,2p), and QCISD/6-311+G(2df,2p) levels of theory.

The quantum chemical calculations carried out in this work were performed by using the GAMESS,<sup>31</sup> Molcas,<sup>32</sup> and Gaussian<sup>33</sup> program packages. The Molden<sup>34</sup> program was also employed to visualize the geometric and electronic features of the different stationary points. The AIM analysis has been carried out by the AIMPAC program.<sup>35</sup>

## Results

Ozone and hydroperoxyl radical are well-known species, and our computed geometrical parameters (Figure 1) are in very good agreement with the experimental data and also with other theoretical results from the literature.<sup>36-39</sup> O<sub>3</sub> has a X<sup>1</sup>A<sub>1</sub> ground state, which is mainly characterized by the combination of the electronic configurations [0.91...5a<sub>1</sub><sup>2</sup>3b<sub>2</sub><sup>2</sup>1b<sub>1</sub><sup>2</sup>6a<sub>1</sub><sup>2</sup>4b<sub>2</sub><sup>2</sup>1a<sub>2</sub><sup>2</sup> - 0.30...5a<sub>1</sub><sup>2</sup>3b<sub>2</sub><sup>2</sup>1b<sub>1</sub><sup>2</sup>6a<sub>1</sub><sup>2</sup>4b<sub>2</sub><sup>2</sup>2b<sub>1</sub><sup>2</sup>]. The b<sub>1</sub> and a<sub>2</sub> orbitals constitute the π system of ozone which confers it its biradical character. HO<sub>2</sub> has a X<sup>2</sup>A'' ground state and is characterized by the electronic configuration [...7a<sup>2</sup>1a''<sup>2</sup>2a''<sup>1</sup>].

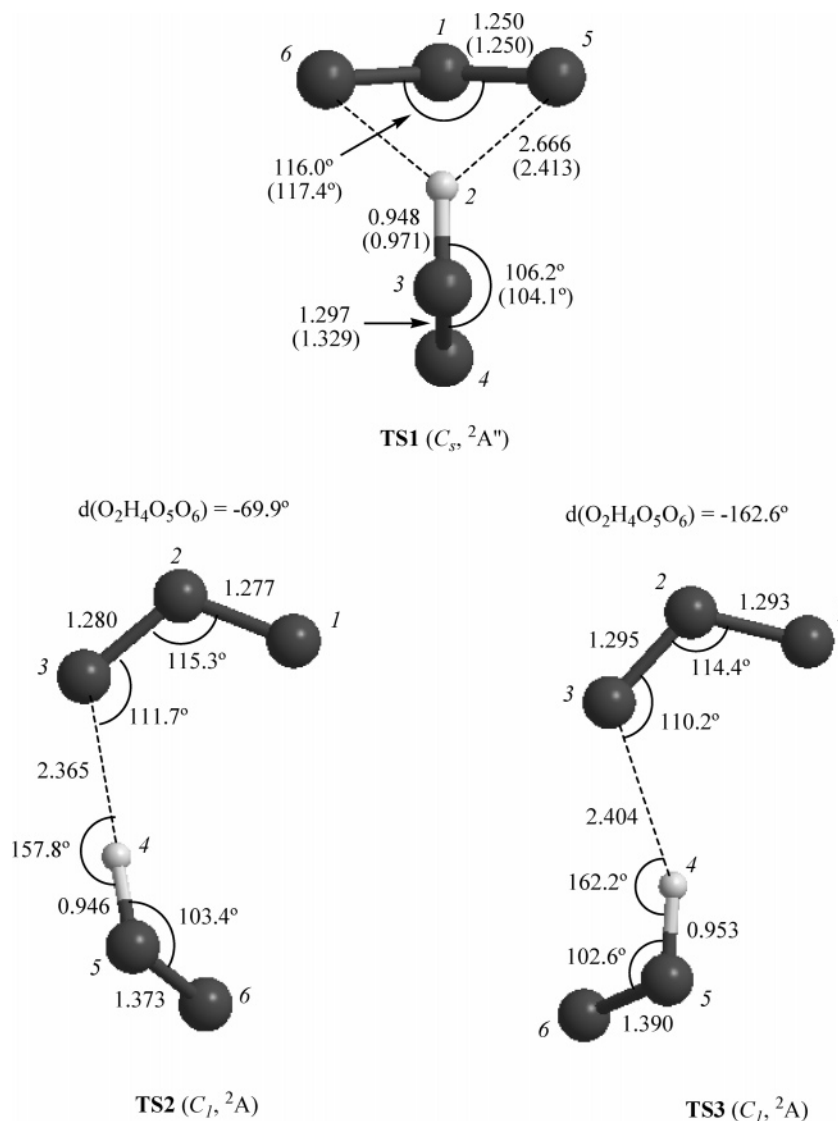


**Figure 2.** Selected geometrical parameters for the stationary points for **TS1**–**TS3** optimized at CASSCF(11,10)/6-311+G(2df,2p) level of theory. The values in parentheses for **TS1** correspond to a QCISD/6-311+G(2df,2p) optimized geometry.

Regarding complexes formed between ozone and hydroperoxyl radical, we have found six stationary points, three of them (named as **C1**, **C2**, and **C3**) correspond to true minima in the potential energy surface whereas the remaining three (designed as **TS1**, **TS2**, and **TS3**) are transition states connecting the mentioned minima. The most relevant geometrical parameters of the stationary points are collected in Figures 1 and 2. A schematic picture of the potential energy surface of these complexes is displayed in Figure 3 and the relative energies of the stationary points are contained in Table 1.

The three minima **C1**, **C2**, and **C3** are formed by the link of one of the terminal oxygens of ozone with the hydrogen of the HO<sub>2</sub> moiety, and the nature of this bond is classified as hydrogen bond according to an AIM analysis of the wave function. Thus, taking the wave function obtained at QCISD level of theory, we have obtained, for the O3...H4 hydrogen bond, a bond critical point (bcp) with the following values of the density ( $\rho_{\text{bcp}}$ ) and the laplacian of the density ( $\nabla^2\rho_{\text{bcp}}$ ): 0.01660 au and 0.06214 au, respectively, for **C1**; 0.030 au and 0.144 au, respectively, for **C2**; and 0.0176 au and 0.0627 au, respectively, for **C3**, and these values are in the range corresponding to typical hydrogen bonds as reported by Koch and Popelier.<sup>40</sup>

From an electronic point of view, the CASSCF calculations show that **C1** ( $C_1$  symmetry,  ${}^2A$ ) is mainly characterized by the combination of the electronic configurations [0.89 (...18a<sup>2</sup>-19a<sup>2</sup>20a<sup>2</sup>21a<sup>1</sup>) - 0.27 (...18a<sup>2</sup>19a<sup>2</sup>21a<sup>1</sup>22a<sup>2</sup>)] whereas **C2** and **C3** (both of  $C_s$  symmetry,  ${}^2A''$ ) are mainly described by the combination of the electronic configurations [0.89 (...16a<sup>2</sup>17a<sup>2</sup>-1a<sup>2</sup>22a<sup>2</sup>3a<sup>2</sup>4a<sup>2</sup>) - 0.29 (...16a<sup>2</sup>17a<sup>2</sup>1a<sup>2</sup>22a<sup>2</sup>4a<sup>2</sup>5a<sup>2</sup>)]. Here, the molecular orbitals 21a of **C1** and 4a'' of **C2** and **C3** are associated with the unpaired electron of hydroperoxyl radical, while the orbitals 20a and 22a of **C1** and 3a'' and 5a'' of **C2** and **C3** correspond to the  $\pi$  system of ozone ( ${}^1a_2$  and  ${}^2b_1$  molecular orbitals of O<sub>3</sub>). Consequently, the electronic structure of the separate reactants is maintained in the formation of the complexes, so that the hydrogen bond interaction involves neither the unpaired electron of HO<sub>2</sub> nor the  $\pi$  system of O<sub>3</sub>.

Regarding the geometrical parameters of the three minima (see Figure 1), the values obtained at QCISD differ utmost in 0.03 Å from those computed at CASSCF level of theory, except for the O...H hydrogen bond which is predicted to be among 0.2–0.3 Å shorter by the QCISD approach than by the CASSCF approach. As pointed out above, this is due to the well-known difficulties of the CASSCF method to describe correctly the hydrogen bond interactions, and therefore, the following discus-

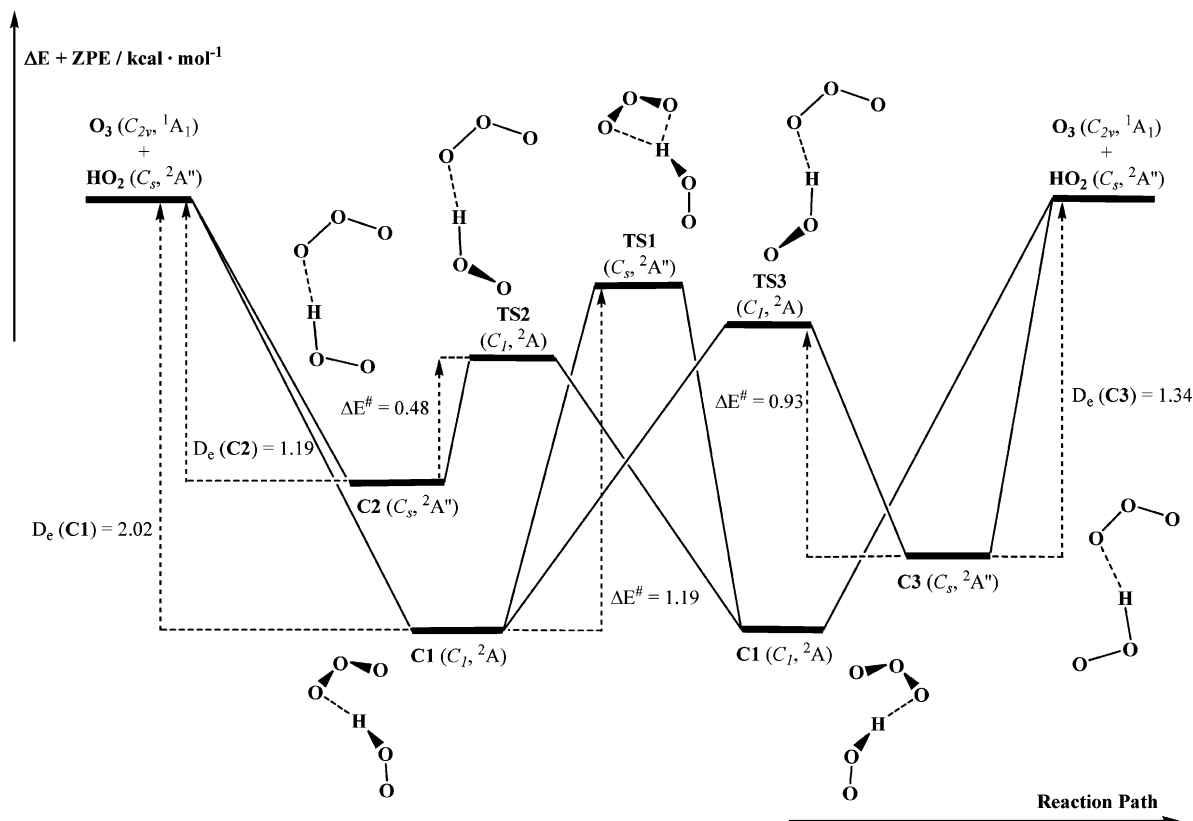


**Figure 3.** Schematic diagram of the potential energy surfaces involving the formation of the C1–C3 hydrogen-bonded complexes.

sion on the geometrical parameters of these minima will be based on the QCISD results. This situation is very similar to that described recently for the  $\text{O}_3 \cdots \text{HO}$  hydrogen bond complex,<sup>13</sup> where the QCISD approach also predicted shorter hydrogen bond distances than the CASSCF approach in the same extent as described in this work.

The most stable hydrogen bond complex is **C1**, in which the  $\text{O}_3$  and  $\text{HO}_2$  moieties are near perpendicular to each other with an angle between the  $\text{OOO}$  and  $\text{HOO}$  planes of  $77.0^\circ$ . The hydrogen of the hydroperoxyl radical points at one of the terminal oxygen atoms of ozone forming a  $\text{O1O2O3H4}$  dihedral angle of  $-25.6^\circ$  (see Figure 1). The hydrogen bond length is predicted to be  $2.123 \text{ \AA}$  and the hydrogen donor angle is computed to be  $141.3^\circ$ . A further CCSD(T) optimization, restricted to the most significant geometrical parameters that affect the hydrogen bond (namely, the hydrogen bond length, the bond between the hydrogen and the donor, and the two angles at the donor and acceptor sites), shows that the triple excitations practically do not affect the geometry of the complex.<sup>42</sup>

In the remaining two minima (**C2** and **C3**), the hydrogen bond interaction occurs also between one of the terminal oxygens of ozone and the hydrogen of the hydroperoxyl moiety, and all atoms are lying in the same plane. In **C2**, the  $\text{OOH}$  moiety is placed in cis with respect to the  $\text{OOO}$  moiety whereas in **C3** it is placed in trans. Otherwise, the geometrical parameters of both complexes are practically the same. In both complexes, the hydrogen bond distance is close to  $2.08 \text{ \AA}$  at QCISD level of theory.

The calculated relative energies have been summarized in Table 1, and the results obtained at CASPT2 and CCSD(T) level differ, at most, in  $0.8 \text{ kcal/mol}$ . The best level of theoretical treatment, namely, CCSD(T)/aug-cc-pVTZ//QCISD/6-311+G(2df,2p), predict **C1**, **C2**, and **C3** to be  $2.02$ ,  $1.19$ , and  $1.34$

**TABLE 1: Imaginary Frequencies (Imag, in  $\text{cm}^{-1}$ ), Zero-Point Energies (ZPE in kcal/mol), Entropies ( $S$  in eu), and Reaction and Activation Energies ( $\Delta E$  in kcal/mol) for the Reaction between  $\text{O}_3$  and  $\text{HO}_2$**

compound	method <sup>a</sup>	imag	ZPE <sup>b</sup>	$S^b$	$\Delta E^c$	$\Delta E + \text{ZPE}^c$
$\text{O}_3 + \text{HO}_2$	C(19,15)		14.2	110.0	0.00	0.00
	CC/QCI		13.0	111.7	0.00	0.00
<b>C1</b> ( $C_1, {}^2A$ )	C(15,13)		14.8	88.1	-2.58	-1.97
					(-1.80)	(-1.19)
	C(19,15) <sup>d</sup>		14.8	88.1	-2.65	-2.04
					(-1.87)	(-1.26)
	CC/QCI		14.7	84.7	-4.46	-2.80
					(-3.68)	(-2.02)
<b>TS1</b>	C(11,10)	-111.6	14.7	72.3	-1.32	-0.85
	<b>C2</b> ( $C_s, {}^2A$ )		14.7	89.6	-1.99	-1.51
					(-1.33)	(-0.85)
	C(19,15)		14.9	89.4	-2.52	-1.86
					(-1.86)	(-1.20)
	CC/QCI		14.5	83.6	-3.30	-1.85
					(-2.64)	(-1.19)
<b>TS2</b>	C(11,10)	-31.4	14.6	81.5	-1.80	-1.38
	<b>C3</b> ( $C_s, {}^2A$ )		14.7	89.3	-2.78	-2.26
					(-2.09)	(-1.57)
	C(19,15)		14.8	88.5	-2.57	-1.96
					(-1.88)	(-1.27)
	CC/QCI		14.5	91.8	-3.48	-2.03
					(-2.79)	(-1.34)
<b>TS3</b>	C(11,10)	-37.7	14.3	86.5	-1.15	-1.03

<sup>a</sup> C(11,10) stands for CASPT2(19,15)/6-311+G(2df,2p)//CASSCF(11,10)/6-311+G(2df,2p); C(15,13) stands for CASPT2(19,15)/6-311+G(2df,2p)//CASSCF(15,13)/6-311+G(2df,2p); C(19,15) stands for CASPT2(19,15)/6-311+G(2df,2p)//CASSCF(19,15)/6-311+G(2df,2p); CC/QCI stands for CCSD(T)/aug-cc-pVTZ//QCISD/6-311+G(2df,2p). <sup>b</sup> The ZPE and  $S$  are computed according to C(11,10) = CASSCF(11,10)/6-311+G(2df,2p); C(15,13) = CASSCF(15,13)/6-311+G(2df,2p); C(19,15) = CASSCF(19,15)/6-311+G(2df,2p); CC/QCI = QCISD/6-311+G(2df,2p). <sup>c</sup> Values in parentheses include BSSE corrections. <sup>d</sup> The ZPE and  $S$  are computed according to C(11,10) = CASSCF(15,13)/6-311+G(2df,2p).

**TABLE 2: Computed Harmonic Vibrational Frequencies (cm<sup>-1</sup>) and Intensities (km·mol<sup>-1</sup>) for O<sub>3</sub>, HO<sub>2</sub>, C1, C, and C3 Calculated at QCISD/6-311+G(2df,2p) Level of Theory<sup>a</sup>**

mode	approx. description	reactants		C1		C2		C3	
		freq.	int.	freq. <sup>b</sup>	int. <sup>c</sup>	freq. <sup>b</sup>	int. <sup>c</sup>	freq. <sup>b</sup>	int. <sup>c</sup>
$\nu_1$	intramolecular twisting			64.0	1.3	38.4	0.4	15.1	1.6
$\nu_2$	intramolecular scissoring			82.0	2.0	49.7	0.6	36.3	1.9
$\nu_3$	intramolecular wagging			97.1	4.9	79.6	0.9	57.2	0.9
$\nu_4$	intramolecular rocking			154.6	12.4	86.7	1.1	99.7	1.2
$\nu_5$	intramolecular HO <sub>2</sub> scissoring			179.0	8.0	142.1	11.4	145.2	6.9
$\nu_6$	intramolecular HO <sub>2</sub> twisting			354.8	66.0	425.1	126.7	407.6	122.8
$\nu_7$	scissoring bending (O <sub>3</sub> )	752.9	5.7	759.5 (6.6)	13.1 (2.3)	752.7 (-0.2)	14.5 (2.6)	761.0 (8.1)	9.6 (1.7)
$\nu_8$	O–O stretching (HO <sub>2</sub> )	1134.8	24.4	962.3 (-172.5)	404.6 (16.6)	940.8 (-194.0)	351.4 (14.4)	973.1 (-161.7)	422.5 (17.3)
$\nu_9$	symmetrical stretching (O <sub>3</sub> )	1005.6	477.7	1144.2 (138.6)	20.8 (0.0)	1142.7 (137.1)	20.6 (0.0)	1142.2 (136.6)	23.9 (0.1)
$\nu_{10}$	asymmetrical stretching (O <sub>3</sub> )	1260.6	0.1	1294.3 (33.7)	30.9 (309.4)	1303.0 (42.4)	33.8 (338.0)	1279.4 (18.8)	18.7 (187.0)
$\nu_{11}$	scissoring bending (HO <sub>2</sub> )	1466.6	41.7	1505.2 (38.6)	62.1 (1.5)	1512.3 (45.7)	28.1 (0.7)	1505.5 (38.9)	22.4 (0.5)
$\nu_{12}$	H–O stretching (HO <sub>2</sub> )	3714.5	36.7	3679.4 (-35.1)	126.4 (3.4)	3695.1 (-19.4)	243.7 (6.6)	3708.8 (-5.7)	272.1 (7.4)

<sup>a</sup> The experimental values are 705, 1042, and 1110 cm<sup>-1</sup> for O<sub>3</sub> and 1098, 1392, and 3436 cm<sup>-1</sup> for HO<sub>2</sub>. <sup>b</sup> Values in parentheses are frequency shifts relative to the monomers. <sup>c</sup> Values in parentheses are the ratios between the intensity of the complex and the corresponding value in the monomer.

**TABLE 3: Rotational Constants (in GHz) for O<sub>3</sub>, HO<sub>2</sub>, and C1–C3, Computed at QCISD/6-311+G(2df,2p) Level of Theory**

	A	B	C
O <sub>3</sub> <sup>a</sup>	113.866	13.752	12.270
HO <sub>2</sub> <sup>b</sup>	623.228	33.625	31.913
C1	9.506	2.756	2.433
C2	9.987	2.149	1.769
C3	9.438	2.610	1.559

<sup>a</sup> The experimental values for O<sub>3</sub> are 106.531, 13.348, and 11.835 GHz.<sup>41</sup> <sup>b</sup> The experimental values for HO<sub>2</sub> are 610.273, 33.518, and 31.667 GHz.<sup>41</sup>

kcal/mol, respectively, more stable than the reactants ( $\Delta E + \text{ZPE}$  values taking into account the BSSE correction). Thus, it turns out that the O<sub>3</sub>···HO<sub>2</sub> complex is slightly more stable than the O<sub>3</sub>···HO complex recently reported in the literature by about 1.00 kcal/mol.<sup>13</sup>

The three transition states (**TS1**, **TS2**, and **TS3**) have been optimized at the CASSCF(11,10) level of theory but **TS1** was also optimized employing the QCISD approach. The most relevant geometrical parameters are displayed in Figure 2. As shown in Figure 3, these transition states connect the different minima described above as it has been determined by the analysis of the transition vector and the IRC (intrinsic reaction coordinate) calculations. Thus, **TS1** corresponds to the transition state linking the two isomers of **C1**, that is, the hydrogen of the HO<sub>2</sub> moiety is linked to each of the terminal oxygens of the O<sub>3</sub> moiety, and the process involves the simultaneous breaking and forming of one hydrogen bond, so that the whole HO<sub>2</sub> moiety is transferred. Figure 2 shows that **TS1** has C<sub>s</sub> symmetry and that the hydrogen atom is equidistant to the two terminal oxygens of the ozone moiety. Also, as pointed out above for the minima, the QCISD approach predicts the hydrogen bond distance that is being formed and broken to be 0.25 Å smaller than that predicted by the CASSCF approach. On the other hand, **TS2** and **TS3** connect **C1** with **C2** and **C1** with **C3**, respectively, in a process that involves a rotation along the O<sub>3</sub>···H<sub>4</sub> hydrogen bond. The energetic barriers for these processes computed at CASPT2//CASSCF level of theory are 1.19 kcal/mol for **TS1**, 0.48 kcal/mol for **TS2**, and 0.93 kcal/mol for **TS3** (see Table 1 and Figure 3). Please note also from Figure 3 that all transition states lie below the energy of the separate reactants.

To help the possible experimental identification of the hydrogen bond complexes described in this work, we report in

Table 2 the computed harmonic vibrational frequencies of **C1**–**C3** along with the ones corresponding to the reactants O<sub>3</sub> and HO<sub>2</sub>. The change in the IR spectra originated by the formation of the hydrogen bond as well as the change of the corresponding intensity is a useful tool to identify experimentally hydrogen bond complexes, as has been done recently for the O<sub>3</sub>···HO complex.<sup>13</sup> Please note that Table 2 contains only the values obtained at QCISD level and correspond to unscaled harmonic frequencies. The IR spectra computed at CASSCF level of theory follow the same trends and are available in the Supporting Information. The results from Table 2 predict that the HO stretching mode is red-shifted by 35.1, 19.4, and 5.7 cm<sup>-1</sup> for **C1**, **C2**, and **C3**, respectively, whereas their intensity is enhanced by 3.4, 6.6, and 7.4 times, respectively. For the remaining vibrational modes, our results predict a blue shift (among 19 and 42 cm<sup>-1</sup>) for the O<sub>3</sub> asymmetric stretching and a red shift (among 162 and 194 cm<sup>-1</sup>) for the OO stretching of the HO<sub>2</sub> moiety.

For a shake of completeness, the rotational constants for the monomers and the complexes are also listed in Table 3. The three complexes are asymmetric rotors and behave like oblate rotors, with  $A > B \approx C$ . The computed rotational constants for ozone and hydroperoxyl radical compare quite well with the experimental values (see footnotes a and b in Table 3).<sup>41</sup>

## Conclusions

The theoretical study carried out in this work has lead us to characterize three hydrogen-bonded complexes (**C1**, **C2**, and **C3**) formed between ozone and hydroperoxyl radical. All of them are held together by one hydrogen bond that is formed between the hydrogen of the HO<sub>2</sub> moiety and one of the terminal oxygens of ozone. The analysis of the corresponding wave function shows that neither the  $\pi$  system of O<sub>3</sub>, which provides its biradical character, nor the unpaired electron of HO<sub>2</sub> participates in the formation of the hydrogen bond. Energy calculations carried out at the best level of treatment, CCSD-(T)/aug-cc-pVTZ, predict these complexes to be 2.02, 1.19, and 1.34 kcal/mol, respectively, more stable than the separate reactants O<sub>3</sub> plus HO<sub>2</sub> at 0 K. We also report computed harmonic vibrational frequencies and rotational constants to help for a possible experimental identification of these complexes.

This work also shows that the three minima are interconnected by three transition states (**TS1**, **TS2**, and **TS2**) that lie also below the energy of the separate reactants.

**Acknowledgment.** The calculations described in this work were carried out at the Centre de Supercomputació de Catalunya

(CESCA), whose services are gratefully acknowledged, and at an AMD Opteron cluster of our group. The financial support for this research was provided by the Spanish Dirección General de Investigación Científica y Técnica (DGYCIT, grant CTQ2005-07790) and by the Generalitat de Catalunya (Grant 2005SGR00111). A. M. thanks the Spanish Ministerio de Educación y Ciencia for a fellowship (BES-2003-1352).

**Supporting Information Available:** This material contains the description of the active spaces used in the CASSCF calculations, absolute energies, Cartesian coordinates for all stationary points, CASSCF vibrational frequencies, and CASSCF rotational constants for the stationary points reported herein. This material is available free of charge via the Internet at <http://pubs.acs.org>.

## References and Notes

- (1) Wayne, R. P. *Chemistry of Atmospheres*, 3rd ed.; Oxford University press: Oxford, U.K., 2000.
- (2) Jacob, D. J. *Introduction to Atmospheric Chemistry*; Princeton University Press: Princeton, NJ, 1999.
- (3) Monks, P. S. *Chem. Soc. Rev.* **2005**, *34*, 376.
- (4) Zahniser, M. S.; Howard, C. J. *J. Chem. Phys.* **1980**, *73*, 1620.
- (5) Sinha, A.; Lovejoy, E. R.; Howard, C. J. *J. Chem. Phys.* **1987**, *87*, 2122.
- (6) Wang, X.; Suto, M.; Lee, L. C. *J. Chem. Phys.* **1988**, *88*, 896.
- (7) David, D.; Nelson, J.; Zahniser, M. S. *J. Phys. Chem.* **1994**, *98*, 2101.
- (8) Nizkorodov, S. A.; Harper, W. W.; Blackmon, B. W.; Nesbitt, D. *J. Phys. Chem. A* **2000**, *104*, 3964.
- (9) Herndon, S. C.; Villalta, P. W.; Nelson, D. D.; Jayne, J. T.; Zahniser, M. S. *J. Phys. Chem. A* **2001**, *105*, 1538.
- (10) Varandas, A. J. C.; Zhang, L. *Chem. Phys. Lett.* **2004**, *385*, 409.
- (11) Varandas, A. J. C.; Zhang, L. *Chem. Phys. Lett.* **2000**, *331*, 474.
- (12) Engdahl, A.; Nelander, B. *J. Chem. Phys.* **2005**, *122*, 126101.
- (13) Mansergas, A.; Anglada, J. M. *ChemPhysChem* **2006**, *7*, 1488.
- (14) Hansen, J. C.; Francisco, J. S. *ChemPhysChem* **2002**, *3*, 833.
- (15) Frisch, M. J.; Pople, J. A.; Binkley, J. S. *J. Chem. Phys.* **1984**, *80*, 3265.
- (16) Hehre, W. J.; Radom, L.; Schleyer, P. v. R.; Pople, J. A. In *Ab Initio Molecular Orbital Theory*; John Wiley: New York, 1986; p 86.
- (17) Roos, B. O. *Adv. Chem. Phys.* **1987**, *69*, 399.
- (18) Anglada, J. M.; Bofill, J. M. *Chem. Phys. Lett.* **1995**, *243*, 151.
- (19) Anderson, K.; Malmqvist, P. A.; Roos, B. O. *J. Chem. Phys.* **1992**, *96*, 1218.
- (20) Pople, J. A.; Head-Gordon, M.; Raghavachari, K. *J. Chem. Phys.* **1987**, *87*, 5968.
- (21) Cizek, J. *Adv. Chem. Phys.* **1969**, *14*, 35.
- (22) Barlett, R. J. *J. Phys. Chem.* **1989**, *93*, 1963.
- (23) Raghavachari, K.; Trucks, G. W.; Pople, J. A.; Head-Gordon, M. *Chem. Phys. Lett.* **1989**, *157*, 479.
- (24) Pople, J. A.; Krishnan, R.; Schlegel, H. B.; Binkley, J. S. *Int. J. Quantum Chem. XIV* **1978**, 545.
- (25) Dunning, T. H. *J. Chem. Phys.* **1989**, *90*, 1007.
- (26) Kendall, R. A., Jr.; Dunning, T. H.; Harrison, R. J. *Chem. Phys.* **1992**, *6769*.
- (27) Lee, T. J.; Taylor, P. R. *Int. J. Quantum Chem. Symp.* **1989**, *23*, 199.
- (28) Rienstra-Kiracofe, J. C.; Allen, W. D.; Schaefer, H. F., III. *J. Phys. Chem. A* **2000**, *104*, 9823.
- (29) Boys, S. F.; Bernardi, F. *Mol. Phys.* **1970**, *19*, 553.
- (30) Bader, R. F. W. *Atoms in Molecules. A Quantum Theory*; Clarendon Press: Oxford, U.K., 1990.
- (31) Schmidt, M. W.; Baldridge, K. K.; Boatz, J. A.; Elbert, S. T.; Gordon, M. S.; Jensen, J. H.; Koseki, S.; Matsunaga, N.; Nguyen, K. A.; Su, S. J.; Windus, T. L.; Dupuis, M.; Montgomery, J. A. *J. Comput. Chem.* **1993**, *14*, 1347.
- (32) Andersson, K.; Barysz, M.; Bernhardsson, A.; Blomberg, M. R. A.; Cooper, D. L.; Fleig, T.; Fülscher, M. P.; DeGraaf, C.; Hess, B. A.; Karlström, G.; Lindh, R.; Malmqvist, P.-Å.; Neogrády, P.; Olsen, J.; Roos, B. O.; Sadlej, A. J.; Schütz, M.; Schimmelpfennig, B.; Seijo, L.; Serrano-Andrés, L.; Siegbahn, P. E.; Stålring, J.; Thorsteinsson, T.; Veryazov, V.; Widmark, P. O. *MOLCAS*, version 6.2 ed.; Lund University: Lund, Sweden, 2005.
- (33) Frisch, M. J.; Trucks, G. W.; Schlegel, H. B.; Scuseria, G. E.; Robb, M. A.; Cheeseman, J. R.; Montgomery, J. A. Jr.; Vreven, T.; Kudin, K. N.; Burant, J. C.; Millam, J. M.; Iyengar, S. S.; Tomasi, J.; Barone, V.; Mennucci, B.; Cossi, M.; Scalmani, G.; Rega, N.; Petersson, G. A.; Nakatsuji, H.; Hada, M.; Ehara, M.; Toyota, K.; Fukuda, R.; Hasegawa, J.; Ishida, M.; Nakajima, T.; Honda, Y.; Kitao, O.; Nakai, H.; Klene, M.; Li, X.; Knox, J. E.; Hratchian, H. P.; Cross, J. B.; Adamo, C.; Jaramillo, J.; Gomperts, R.; Stratmann, R. E.; Yazyev, O.; Austin, A. J.; Cammi, R.; Pomelli, C.; Ochterski, J. W.; Ayala, P. Y.; Morokuma, K.; Voth, G. A.; Salvador, P.; Dannenberg, J. J.; Zakrzewski, V. G.; Dapprich, S.; Daniels, A. D.; Strain, M. C.; Farkas, O.; Malick, D. K.; Rabuck, A. D.; Raghavachari, K.; Foresman, J. B.; Ortiz, J. V.; Cui, Q.; Baboul, A. G.; Clifford, S.; Cioslowski, J.; Stefanov, B. B.; Liu, G.; Liashenko, A.; Piskorz, P.; Komaromi, I.; Martin, R. L.; Fox, D. J.; Keith, T.; Al-Laham, M. A.; Peng, C. Y.; Nanayakkara, A.; Challacombe, M.; Gill, P. M. W.; Johnson, B.; Chen, W.; Wong, M. W.; Gonzalez, C.; Pople, J. A. *Gaussian 03*, Revision C.01; Gaussian, Inc.: Wallingford, CT, 2004.
- (34) Shaftenaar, G.; Noordik, J. H. *J. Comput.-Aided Mol. Des.* **2000**, *14*, 123.
- (35) Bader, R. F. W. AIMPAC. <http://www.chemistry.mcmaster.ca/aimpac> (accessed May 2002).
- (36) Herzberg, G. *Electronic Spectra and Electronic Structure of Polyatomic Molecules*; Van Nostrand Reinhold Co.: New York, 1966.
- (37) Banichevich, A.; Peyerimhoff, S. D. *Chem. Phys.* **1993**, *174*, 93.
- (38) Borowski, P.; Andersson, K.; Malmqvist, P.-Å.; Roos, B. O. *J. Chem. Phys.* **1992**, *97*, 5568.
- (39) Borowski, P.; Fülscher, M.; Malmqvist, P.-Å.; Roos, B. O. *Chem. Phys. Lett.* **1995**, *237*, 195.
- (40) Koch, U.; Popelier, P. *J. Phys. Chem.* **1995**, *99*, 9747.
- (41) NIST Standard Reference Database no. 69, March 2003 ed.; <http://webbook.nist.gov/chemistry>, June 2005.
- (42) The CCSD(T)/6-311+G(2df,2p) optimized geometrical parameters for C1 are  $d(\text{O3H4}) = 2.120 \text{ \AA}$ ,  $d(\text{H5O5}) = 0.976 \text{ \AA}$ ,  $A(\text{O2O3H4}) = 107.1^\circ$ , and  $A(\text{O3H4O5}) = 139.6^\circ$ .